Investigation of the Equilibrium $N_2O_4 \rightleftharpoons 2NO_2$ by Electron Diffraction: Molecular Structures and Effective Temperature and Pressure of the Expanding Gas with Implications for Studies of Other Dimer−Monomer Equilibria

Quang Shen[†] **and Kenneth Hedberg***

Department of Chemistry, Oregon State University, Corvallis, Oregon 97331

Received: February 25, 1998; In Final Form: May 5, 1998

Gas-phase electron-diffraction patterns are obtained from jets that are expanded into a vacuum. Knowledge of the effective temperature of the sample in the diffraction zone is essential for reliable analyses of any equilibria that may exist between different species and for an understanding of the vibrational properties of the molecules. Knowledge of the effective pressure is also essential for analyses of equilibria in which the number of molecules changes during reaction. The temperature and pressure dependence of the equilibrium $N_2O_4 \rightleftharpoons 2NO_2$ was studied to investigate these matters. The diffraction experiments fall into two sets: (1) those with nozzle temperatures of 104, 25, 2, −12, −25, and −35 °C with the sample bath temperature constant at −43 °C and (2) those with the nozzle temperature constant at −12 °C and bath temperatures of −26, −36, and −43 °C. The amount of N_2O_4 was found to range from 76.3 (29)% with the bulk sample at −43 °C and the nozzle tip at −35 °C to zero with the nozzle tip at 104 °C. Analysis of the temperature dependence of the equilibrium reveals that effective temperature in the diffraction zone is satisfactorily represented by the formula $T = aT_{nt}$, where T_{nt} is the nozzle-tip temperature and $a = 0.980$ ($\sigma = 0.098$). Thus, for $T_{nt} = 300$ K one has $T = 294$ K ($\sigma = 29$); however, there is evidence that the magnitude of the uncertainty is too conservative and that a more likely figure is 10−15 K. A similar analysis of the effective pressure based on the formula $P_t = bP_{bs}$, where P_{bs} is the vapor pressure of the bulk sample determined by the temperature of the sample bath, led to a plausible but very imprecise value for b: 0.56 (148). The values of both a and b are in principle dependent on nozzle geometry, but in view of its imprecision the matter is moot for b. Our value for a should be applicable to most gas-phase electron-diffraction nozzles in current use, i.e., nozzles having a ratio of capillary length to diameter greater than 10−15. It should also be applicable to the separate components of gaseous system and to equilibria that become established in the nozzle system. The structures of the molecules are in excellent agreement with those measured earlier. Results (r_a/Å; $\angle_\alpha$/deg) with estimates of 2σ uncertainties are as follows. N_2O_4 at $T_{nt} = -35$ °C: r(N═O) = 1.191 (1), r(N−N) = 1.774 (5), ∠O═N═O = 134.8 (4). NO_2 at $T_{nt} = 104$ °C: r(N═O) = 1.199 (1), ∠O═N═O = 134.8 (4).

Introduction

Electron diffraction (GED) has been used in a series of investigations from this and other laboratories to study gas-phase systems of rotational conformers at different temperatures.[1,2] In addition to the usual structure measurements, a major aim of these studies was the evaluation of the conformational energy and entropy differences through the temperature dependence of the equilibrium constants (in this case determined only by the mole ratios) given by the well-known formula

$$-RT \ln K_p = \Delta G^\circ = \Delta H^\circ - T\Delta S^\circ \qquad (1)$$

Because the GED experiment occurs in a jet of gas that is being expanded into high vacuum from a nozzle with a fine tip, questions have been raised about the appropriate temperature of the sample. Indeed, theoretical study[3] indicates that this temperature could be quite different from that of the nozzle tip through which the sample passes. On the other hand, the significant changes in composition observed from modest temperature changes of the nozzle in the many studies of conformational equilibria leave no doubt that these changes are consistent with an effective sample temperature close to that of the nozzle tip. There is also modest theoretical justification for this result,[4] and implicit support for it exists in the good agreement usually found between the temperature-dependent observed and calculated amplitudes of vibration.

The analysis of a system of rotational conformers is simple because conformational equilibria are established on a very short time scale relative to the dynamics of sample transport through the nozzle and because interconversion of conformers leads to no change in the number of molecules; the latter is especially important since the mole ratio, which is the composition parameter measured in a GED experiment, is pressure independent. Extension of the diffraction method to systems where the number of molecules changes in the course of reaction presents a much more difficult problem in two ways. The first is the nature of the system itself. To obtain the desired information, equilibrium must be reached in the course of sample transit through the nozzle in order that the measurable constants of the experiment (nozzle-tip temperature and bulk-sample pressure) have relevance. Second, since the method measures the relative *numbers* of molecules of different types, the equilibrium constant in terms of mole fractions now contains a pressure factor, as is seen in the usual formula applicable to

[†] Department of Chemistry, Colgate University, Hamilton, NY 13346.

S1089-5639(98)01297-3 CCC: $15.00
Published on Web 07/17/1998

the dissociation of a dimeric substance, $D \rightleftharpoons 2M$:

$$K_p = \frac{X_M^2}{X_D} P_t \qquad (2)$$

Inasmuch as the GED experiment occurs in a jet of gas that is being expanded into high vacuum, the appropriate value for the total pressure P_t is not obvious.

Many years ago we became interested in extending our work on conformational equilibria to systems in which the reactions are accompanied by a formal volume change. The simplest are the dissociation equilibria mentioned in connection with eq 2, and several of the type $M_2X_6 \rightleftharpoons 2MX_3$, M = Al, Ga; and X = Cl, Br, I were investigated[5] as well as the equilibrium $N_2O_4 \rightleftharpoons 2NO_2$. As implied above, the major problem concerning the thermodynamics of these systems is the effective value of the system pressure P_t: how it might be estimated from known quantities such as the nozzle-tip temperature T_{nt} and the vapor pressure of the bulk sample P_{bs}. To answer this question, it is necessary to examine a system for which the pressure and temperature dependence of the equilibrium is well-known in order to provide a reliable basis for the interpretation of the diffraction results. The composition of such a system must also be capable of large variation over the temperature range applicable to the problem, the different system components must be as few as possible, the equilibrium must be established very rapidly at all temperatures, and the constituent molecules must have simple structures. The equilibrium $2NO_2 \rightleftharpoons N_2O_4$ meets all of these requirements for the investigation of P_t and at the same time affords opportunity for additional verification of the customary assumption that the nozzle-tip temperature represents well the effective temperature of the molecules in the scattering region. Our early unpublished work[5] on this system provides insights on both the effective sample temperature and pressure for this monomer−dimer type equilibrium. Because this study has relevance to our current studies of similar types of equilibria, we decided the results merit the formal presentation that appears here.

Experimental Section

Nitrogen dioxide (99.5%)was obtained from Matheson Gas Products. Material was distilled into a sample container from a cold trap which had been filled from the original cylinder. Before loading the sample container the material in the cold trap was pumped for several hours while being maintained at −80 °C. During the diffraction experiments the vapor pressure of the sample was controlled by immersing its container external to the diffraction apparatus in a dry ice−acetone bath. The temperature of the bath was measured by a thermometer and carefully adjusted by adding appropriate amounts of dry ice. The nozzle consisted of two concentric tubes: a central tube (Monel) connected to the sample container and fitted with a tip about 10 mm long and 0.3 mm in diameter and an outer tube sealed to the inner one close to the tip. A long probe inserted in the annular space between the tubes served to introduce a stream of heated or cooled nitrogen gas close to the nozzle tip, which then flowed back along the assembly before being vented. The temperature of the nozzle was measured with a thermocouple fastened to the nozzle tip and maintained by adjusting the flow and temperature of the nitrogen gas. The distance between the undiffracted electron beam and the nozzle tip was about 1 mm.

The ED photographs were made in the OSU apparatus using a rotating sector with angular opening approximately equal to r^3 and using 8 × 10 in. Kodak projector slide (medium contrast) plates developed in D19 developer for 10 min. Other experimental conditions are as follows: nominal camera distances, 750 cm (long camera, LC) and 300 cm (middle camera, MC); nominal accelerating potential 40 kV, calibrated against CO_2 (r_a(C═O) = 1.1642 Å and r_a(C··O) = 2.3244 Å) in separate experiments; electron-beam currents, 0.38−0.44 μA; exposure times, 1−5 min; ambient pressure in the main chamber during sample run-in, (2.6−7.0) × 10^{-6} Torr; nominal ranges of data, 2.0 ≤ s/Å ≤ 13.0 (LC) and 8.0 ≤ s/Å ≤ 31.0 (MC).

The experiments fall into two groups. One group was designed to measure the effect of nozzle temperature (i.e., temperature of the vapor) at constant bulk-sample vapor pressure on the composition of the gas; the other, to measure the effect of vapor pressure on the gas composition at constant nozzle temperature. The first group of experiments was made with nozzle-tip temperatures (T_{nt}) of 104, 25, 2, −12, −25, and −35 °C with the sample bath maintained at −43 °C. The second group of experiments was made with the nozzle-tip temperature at −12 °C and sample bath (bulk sample) temperatures (T_{bs}) of −26, −36, and −43 °C. Four plates from each of these experiments (two each from the LC and MC) were selected for analysis. The procedures for obtaining the molecular intensities have been described.[6] The scattering factors used in these and other calculations were obtained from tables.[7] The experimental intensities from each plate and details of the experimental conditions are found in the Supporting Information.

Data Analysis

Structures and Compositions of the Mixtures. The radial distribution curves for the mixtures seen in Figure 1 show clearly the changing degree of decomposition of N_2O_4 with increasing temperature at a constant bulk sample pressure, and the shift in the equilibrium with changing bulk sample pressure at constant tempereature. Because the r_a structures of both NO_2[5,8] and N_2O_4[9] are well-known, the principal aim of the work was the measurement of the compositions. However, these were expected to be correlated with the structures of the components, which required careful attention to the latter as well.

Since N_2O_4 is known to have D_{2h} symmetry[9] (and NO_2 to have C_{2v}), the model of the mixture is completely described by two structural and two vibrational parameters for NO_2, three structural and six vibrational parameters for N_2O_4, and a composition parameter. For convenience these were chosen to be r_m(N═O), r_m(O·O), l_m(N═O), and l_m(O·O) for the monomer and r_d(N═O), r_d(N−N), $\angle_d$ONO, l_d(N═O), l_d(N−N), l_d(N·O), l_d(O·O), l_d(O··O_{cis}), and l_d(O··O_{trans}) for the dimer; diagrams of the molecules are seen in Figure 2. Since the structures of NO_2 itself and the $-NO_2$ group in N_2O_4 are so similar, high correlations among parameters required some assumptions. The most important assumption was that the structure of NO_2 is not significantly affected by the temperature differences in our experiments, i.e., that the structure found at 104 °C where it was the only species present could be introduced as a constraint, if desired, in the mixtures.

For each experiment the refinements were carried out by a least-squares fitting of a theoretical intensity curve simultaneously to the four data sets.[10] Refinement of a model consisting of NO_2 only with use of the 104 °C data proceeded smoothly to convergence. Analyses of the remaining systems were carried out as follows. For the refinements based on the low-temperature experiments (nozzle tip at 2, −12, −25, and −35 °C) where the population of N_2O_4 dominated, the NO_2 distances as obtained at 104 °C were included as constrained

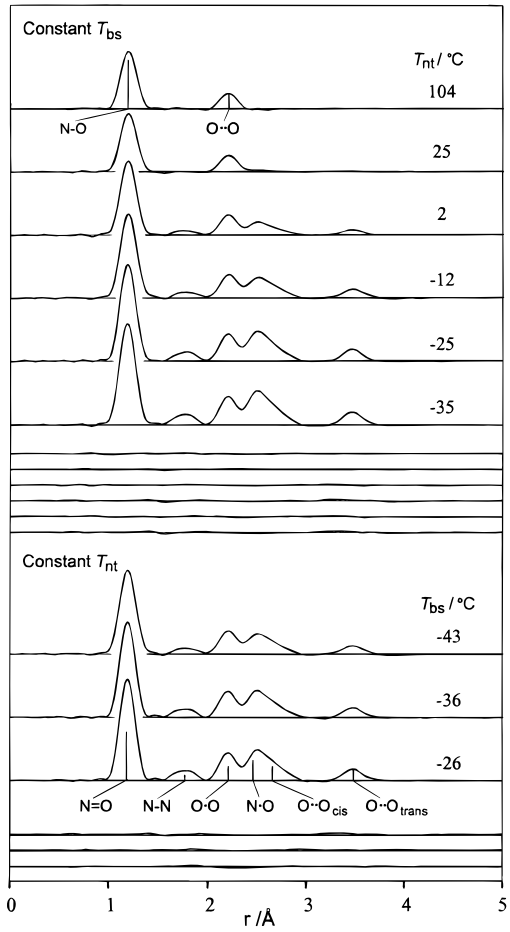

Figure 1. Radial distribution curves for mixtures of NO_2 and N_2O_4 under different conditions of nozzle-tip temperature, T_{nt}, and bulk-sample temperature, T_{bs}. The curve for $T_{nt} = 104$ °C is for pure NO_2; and that for $T_{bs} = -26$ °C, for essentially pure N_2O_4. The vertical lines under the peaks have lengths proportional to the weights of the labeled terms. Corresponding difference curves (experimental minus theoretical) are shown under each group.

quantities. The vibrational amplitudes of the NO_2 molecules were tied to those of the corresponding distances in N_2O_4 and refined with them as a group. The other geometrical as well as the vibrational parameters of N_2O_4 and the mole fraction parameter (χ_d) refined smoothly. The mixture at 25 °C comprised more than 90% NO_2, and since the structure of the remaining small amount of N_2O_4 could not be reliably refined, its structure had to be assumed and constrained. None of the other experiments yielded a mixture composition corresponding to pure N_2O_4; however, the results for its structure from the lowest temperatures (−35 and −25 °C) were judged to be significantly accurate to permit their use as known quantities in the analysis of the 25 °C data. For this refinement only the four NO_2 parameters and the composition parameter were varied. The final results for all systems are given in Tables 1 and 2.

The consistency of the geometrical parameters resulting from these studies is excellent. Either of the sets of results from the 104 and 25 °C refinements shown in Table 1 is a satisfactory description of the structure of NO_2, and the results from any of the refinements from the lower temperatures are satisfactory descriptions of the structure of N_2O_4. All values are in good agreement with those reported earlier[8,9,11] (Table 3). Intensity curves for these systems are seen in Figure 3, and the correlation matrix for the parameters of N_2O_4 at −42 °C is given in Table 4.

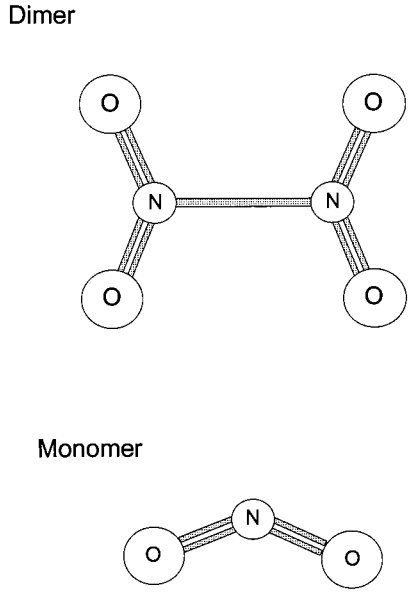

Figure 2. Diagrams of the N_2O_4 and NO_2 molecules.

Effective Nozzle-Tip Temperature and Sample Pressure. We assume that P_t is proportional to the vapor pressure of the bulk sample P_{bs} and the effective temperature to the Kelvin temperature of the nozzle tip T_{nt}:

$$P_t = bP_{bs}; \quad T = aT_{nt} \tag{3}$$

Substitution of eqs 2 and 3 into eq 1 and rearranging, we obtain

$$-R \ln\left[\frac{X_{NO_2}^2}{X_{N_2O_4}} P_{bs}\right] = \frac{\Delta H^\circ}{aT_{nt}} - \Delta S^\circ + R \ln b \tag{4}$$

Equation 4 indicates that elucidation of the temperature and pressure dependence of the system composition will reveal $\Delta H^\circ/a$ and $\Delta S^\circ - R \ln b$ for the $N_2O_4 \rightleftharpoons 2NO_2$ reaction. Comparison with the known values of the enthalpy and entropy differences obtained by other methods will yield values for a and b if the vapor pressure of the bulk sample, P_{bs}, can be satisfactorily estimated. Since the diameter of the nozzle tip itself is small compared with the diameter of the tube that conveys the sample gas to the tip, we may safely assume that P_{bs} is determined by T_{bs}. It may then be calculated from the formula[12]

$$\log P_{bs,cmHg} = -2460.0/T_{bs} + 9.58149 + 7.612172 \times 10^{-3} T_{bs} - 1.51335 \times 10^{-5} T_{bs}^{\ 2} \tag{5}$$

Figure 4 shows a plot of eq 4 with use of our GED values for the compositions and the values of P_{bs} calculated from eq 5 together with a straight line (dashed) fitted to them by least squares. Also plotted for comparison are results from pressure measurements,[13] from spectroscopy[14] and from calculations based on a variety of earlier measurements[15] and a least-squares straight line (solid) fitted to the three sets of data. The last has a slope (ΔH°) and associated standard deviation equal to 13.52 (4) kcal·mol^{-1}·deg^{-1} and an intercept, $-\Delta S^\circ$, of −41.52 (14) cal·mol^{-1}. The slope of the curve from our GED results, $\Delta H^\circ/a$, is seen to be in excellent agreement with that from the other methods; indeed, its value of 13.80 (138) kcal·mol^{-1}·deg^{-1} lies well within the associated uncertainties. If the 13.52 kcal·mol^{-1}·deg^{-1} value for ΔH° is accepted as correct, the result

TABLE 1: Structural Results from Experiments at Different Nozzle-Tip Temperatures with Constant Bulk-Sample Pressure[a,b]

nozzle temp/°C:	104	25	2	−12	−25	−35
bath temp/°C	−38	−40	−43	−43	−43	−43
			Monomer			
r(N═O)	1.199(1)	1.198(2)	[1.199]	[1.199]	[1.199]	[1.199]
r(O·O)	2.207(4)	2.205(4)	[2.207]	[2.207]	[2.207]	[2.207]
∠O═N═O	134.0(5)	133.9(5)	[134.0]	[134.0]	[134.0]	[134.0]
l(N═O)	0.0416(21)	0.046(2)[c]	0.043(2)[c]	0.046(2)[c]	0.042(2)[c]	0.044(2)[c]
l(O·O)	0.0530(37)	0.057(4)[d]	0.055(4)[d]	0.055(4)[d]	0.052(3)[d]	0.050(3)[d]
			Dimer			
% dimer (α_D)	0	4.5(20)	30.3(50)	49.7(86)	68.2(51)	76.3(82)
r(N═O)		[1.192]	1.191(2)	1.194(2)	1.193(1)	1.191(2)
r(N−N)		[1.773]	1.772(11)	1.773(11)	1.775(4)	1.774(5)
∠O═N═O		[134.5]	134.4(9)	134.5(8)	134.7(3)	134.8(4)
r(O·O)		[2.199]	2.195(7)	2.201(6)	2.202(3)	2.199(4)
r(N·O)		[2.490]	2.489(8)	2.491(8)	2.491(4)	2.488(5)
r(O··O_{cis})		[2.695]	2.696(14)	2.697(13)	2.694(5)	2.689(7)
r(O··O_{trans})		[3.478]	3.477(9)	3.481(9)	3.479(5)	3.473(5)
l(N═O)		0.046(2)[c]	0.044(2)[c]	0.046(2)[c]	0.042(2)[c]	0.044(2)[c]
l(N−N)		[0.072]	0.069(20)	0.087(21)	0.077(8)	0.074(10)
l(O·O)		0.057(4)[d]	0.055(4)[d]	0.055(4)[d]	0.052(3)[d]	0.050(3)[d]
l(N·O)		[0.073]	0.077(10)	0.085(10)	0.079(5)	0.079(6)
l(O··O_{cis})		[0.100]	0.099(21)	0.102(19)	0.102(8)	0.101(8)[e]
l(O··O_{trans})		[0.075]	0.077(16)	0.080(15)	0.073(6)	0.076(7)[e]
R[f]	0.0674	0.0749	0.0766	0.0902	0.0441	0.0642

[a] Distances (r_a, equal to $r_g - \langle l^2 \rangle / r$), and rms amplitudes ($l$) in angstroms, angles $\angle_\alpha$ in degrees. [b] Values in parentheses are estimates of 2σ uncertainties; those in square brackets were not refined. [c] Refined together as a group. [d] Refined together as a group. [e] Refined together as a group. [f] $R = [\sum w_i \Delta_i^2 / (\sum w_i I_i^2(\text{obs}))]^{1/2}$ where $\Delta_i = I_i(\text{obs}) - I_i(\text{calc})$.

TABLE 2: Structural Results from Different Bulk-Sample Pressures with Nozzle Tip at −12 °C[a]

bath temp/°C:	−26		−36		−43	
nozzle temp/°C:	−12		−12		−12	
	r_a	l	r_a	l	r_a	l
			Monomer			
N═O	[1.199]	0.038(2)[b]	[1.199]	0.038(2)[b]	[1.199]	0.046(2)[b]
O·O	[2.207]	0.047(3)[c]	[2.207]	0.048(3)[c]	[2.207]	0.055(5)[c]
∠O═N═O	[134.0]		[134.0]		[134.0]	
			Dimer			
% dimer (α_D)	71.6(60)		61.5(71)		49.7(86)	
N═O	1.192(1)	0.038(2)[b]	1.193(2)	0.038(2)[b]	1.194(2)	0.046(2)[b]
N−N	1.771(4)	0.076(8)	1.767(6)	0.073(11)	1.773(11)	0.087(21)
∠O═N═O	134.3(3)		134.1(4)		134.5(8)	
O·O	2.197(3)	0.047(3)[c]	2.197(4)	0.048(3)[c]	2.201(6)	0.055(5)[c]
N·O	2.489(4)	0.082(5)	2.488(5)	0.079(6)	2.491(8)	0.085(10)
O··O_{cis}	2.697(6)	0.099(8)	2.697(8)	0.099(12)	2.697(13)	0.102(19)
O··O_{trans}	3.478(5)	0.084(7)	3.479(6)	0.083(10)	3.481(9)	0.080(15)
R	0.0453		0.0625		0.0902	

[a] See footnotes to Table 1.

is $a = 0.980$ (98). For our experiments the actual temperatures applicable to the gaseous sample are thus about 5 K lower than the nominal values with uncertainties (1σ) of about 25 K.

Unfortunately, the method is not so successful in the case of the effective pressure because of the long extrapolation to the zero value of $1/T$. The intercept of the GED curve from Figure 4 has the value −42.68 (526) (equal to $-\Delta S^\circ + R \ln b$), which with the ΔS° value given above leads to $b = 0.56$ (148). Although the indicated effective sample pressure of a little more than half the vapor pressure of the bulk sample is quite plausible, the large uncertainty indicates that this factor is not reliable. This is seen graphically in Figure 5, which is a plot of the function

$$\frac{K_P X_D}{(1 - X_D)^2} = b P_{bs} \tag{6}$$

obtained by rearrangement of the expression for the equilibrium constant

$$K_P = \frac{(1 - X_D)^2}{X_D} b P_{bs} \tag{7}$$

in terms of the quantities of our system: P_{bs} is calculated from eq 5 and the bulk sample temperature, X_D is from the GED results, and K_P is taken from the results of the other methods adopted as our standard. The dashed curve reflects the use of the K_P value at 261 K and has a slope $b = 1.032$ (23). This is remarkably close to unity and suggests that if 261 K were to represent the effective temperature of the gas in the scattering region, the effective pressure in this region is essentially that of the bulk sample, which is obviously quite unlikely. The solid curve invokes the result of the analysis of effective temperature; that is, it is presumed that the real temperature is only 98.0% of the nozzle-tip value, or 256 K. The slope of this curve is $b = 0.606$ (35), indicating the effective pressure to be only about half that of the bulk sample. It is pleasing that this value for b and the 0.56 (148) obtained with use of eq 4 are consistent since they are derived from different sets of data.

TABLE 3: Structural Parameter Values from Different Investigations of NO_2 and N_2O_4

	NO_2		
r(N═O)/Å	1.199(1)	1.202(3)	$1.193_4(1_0)$
∠O═N═O/deg	134.0(5)	134.0(10)	$134.0_7(1_0)$
method	ED[a]	ED[a]	MW[b]
reference	this work	8	10
	N_2O_4		
r(N═O)/Å	1.191(2)	1.190(2)	
r(N−N)/Å	1.774(5)	1.782(8)	
∠O═N═O/deg	134.8(4)	135.4(6)	
method	ED[a]	ED[a]	
reference	this work	9	

[a] r_a type distances. [b] r_s type distances.

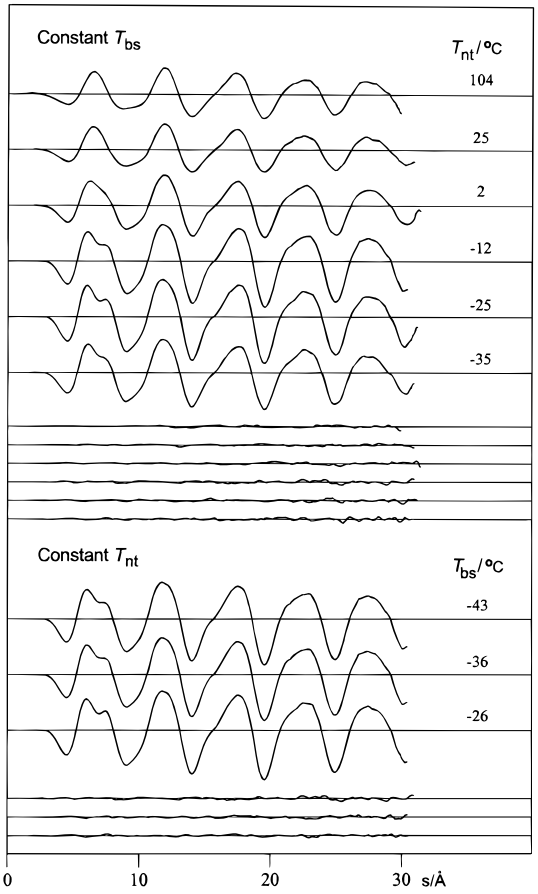

Figure 3. Composite intensity curves for mixtures of NO_2 and N_2O_4 under different conditions of temperature and pressure. See legend to Figure 1.

Discussion

The structures of the molecules NO_2 and N_2O_4 have been briefly discussed in an earlier section and need no further mention here. Apart from these, there are two important results of our study of the $NO_2-N_2O_4$ system. First, the effective temperature—the temperature T (eq 3) that determines the equilibrium constant—is very close to that measured at the tip of the nozzle capillary through which the material passes as it expands into the diffraction chamber, and second, the effective pressure of the system is roughly only about half that determined by the temperature of the solid sample. The values of a and b are obviously correlated, but from the nature of the intercepts of the curves from Figure 4 (equal to $\Delta S° + R \ln b$) and the slopes of those from Figure 5 (equal to b) the value of a is much less affected by b than vice versa. For example, the range of the intercepts varies only from about −41 to −46 due to the practical limits on b, which with the long extrapolation can lead to only a small change in the slope and thus to small changes in a, whereas b is seen from eq 7 to be proportional to K_P, which is very sensitive to temperature. This circumstance accounts for the large differences in the uncertainties attached to a and b obtained by regression analysis of the curve represented by eq 4. However, there is reason to believe that the uncertainty of 10% attached to a from the regression analysis may in fact be overstated. We have calculated from eq 4 the apparent sample temperatures obtained with use of the presumably accurate $\Delta H°$ and $\Delta S°$ values from the other studies cited earlier and our measured mole ratios assuming values of b in the range 0.1−0.9. The results from 25 different combinations differ from the corresponding nozzle-tip temperatures by a maximum of 27 K and on average by only 9 K. For b values assumed to lie in the likely range 0.25−0.5 the maximum difference is 18 K and the average value 10 K. One may conclude that for temperatures normally encountered in GED work, the effective sample temperature is about 98% of that measured at the nozzle tip with an uncertainty of about 5%.

The reason for the small drop in temperature lies in the low sample vapor pressures, usually about 10 Torr, and the geometry of the nozzle system, the capillary tip of which has a cross section about 20 times smaller than that of the main nozzle tube leading from the sample container. As the gas passes into the capillary, it experiences an increase in translational kinetic energy under essentially adiabatic conditions, which leads to an initial temperature drop. Most of the drop is negated by collisions with the capillary walls during passage of the gas through the capillary, but expansion into the high-vacuum region of the apparatus leads to some additional Joule−Thomson cooling. However, since the sample vapor pressure is low, this second drop in temperature is small. The effective temperature is thus set by conditions at some undetermined point upstream from the scattering region. The effective pressure is similarly set by upstream conditions. It may be regarded as the pressure that prevails when the equilibrium is effectively frozen during sample gas expansion.

The meaning of effective temperature and pressure in a nonequilibrium situation such as that occurring in GED experiments is a subtle matter, but in the present case T may be identified with the translational temperature T_{tr} that determines the equilibrium constant and the effective pressure with the total pressure P_t that applies to the system under the temperature circumstance just mentioned and the bulk sample vapor pressure P_{bs}. The vibrational temperature T_{vib} is important in connection with amplitudes of vibration which are also measured in GED work and could in principle be quite different from T_{tr}. However, our estimates[4] of T_{vib} for material passing through nozzles of the type generally used in GED work do not differ much from the nozzle-tip temperature itself, which as noted in the Introduction is consistent with experience based on amplitude measurements obtained over many years. Accordingly, we believe that T, T_{tr}, and T_{vib} do not differ significantly in most cases.[16] Unlike the small temperature difference $T_{nt} - T$, the difference between the vapor pressure of the solid sample P_{bs} and the pressure P_t that applies to the equilibrium in the scattering region is large.

The first-order rate of decomposition of N_2O_4 is known to be very fast with rate constants estimated[17] in the range $15 < k/s < 6 \times 10^4$ for temperatures $258 < T/K < 298$; the corresponding half-lives are $0.05 < t/s < 1 \times 10^{-5}$. Rough estimates of the residence time of the $NO_2-N_2O_4$ sample in the main part of our nozzle assembly and in the capillary portion

TABLE 4: Correlation Matrix (×100) for the $NO_2-N_2O_4$ System from Experiments with Nozzle Tip at −12 °C and Bulk Sample at −43 °C

	parameter[a]	σ_{LS}[b] × 100	r_1	r_2	r_3	r_4	r_5	r_6	$\angle_7$	l_8	l_9	l_{10}	l_{11}	l_{12}	l_{13}	α_{14}
1	r_d(N═O)	0.060	100	−36	−9	<1	30	40	−43	−2	13	−16	29	10	20	45
2	r_d(N−N)	0.38		100	46	79	12	36	60	−2	−11	9	−12	1	−10	−19
3	r_d(O·O)	0.20			100	<1	−63	−31	9	4	4	<1	−10	−10	−4	−11
4	r_d(N·O)	0.27				100	70	85	<1	5	−10	3	5	13	1	6
5	r_d(O··O_{cis})	0.43					100	94	−72	−6	−5	−4	20	19	11	27
6	r_d(O··O_{trans})	0.28						100	49	−6	−4	19	20	19	11	28
7	∠O═N═O)	27.0							100	4	−3	8	−23	−14	−14	−32
8	l_d(N═O)	0.050								100	14	18	0	1	2	−7
9	l_d(N−N)	0.75									100	−5	22	14	13	29
10	l_d(O·O)	0.14										100	−29	−19	−11	−26
11	l_d(N·O)	0.33											100	60	30	67
12	l_d(O··O_{cis})	0.65												100	19	32
13	l_d(O··O_{trans})	0.51													100	39
14	α_d[c]	3.1														100

[a] For the dimer. Monomer parameters were tied to those of the dimer. [b] Standard deviations from least squares. Distances (r) and amplitudes (l) in angstroms; angles (∠) in degrees. [c] Percent dimer.

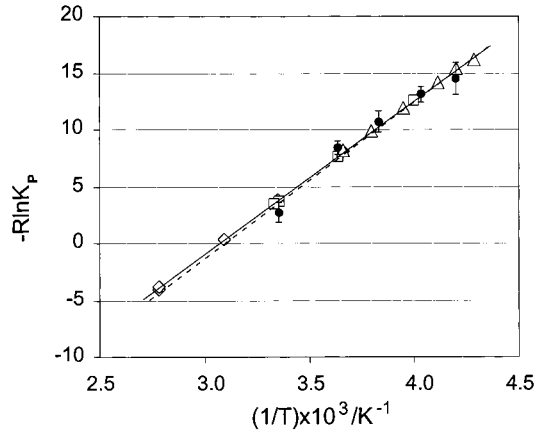

Figure 4. Van't Hoff plot of data for equilibrium mixtures of NO_2 and N_2O_4. Data from following sources. (◇) ref 13; (△) ref 14; (□) ref 15; (●) this work; error bars are estimated 2σ. Lines are least-squares fits; solid line to the data of the three references, dashed to this work.

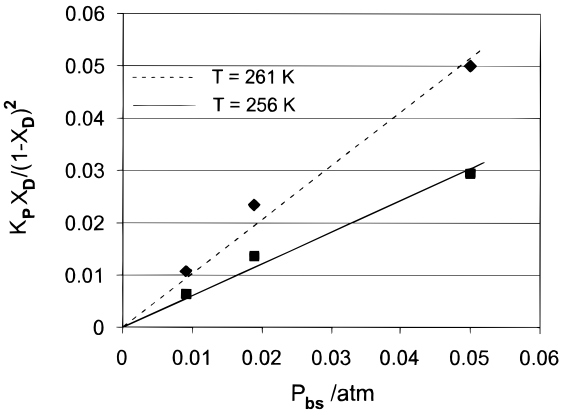

Figure 5. Least-squares plots of the function $K_P X_d/(1 - X_d)^2 = bP_{bs}$ for two assumed effective temperatures. The K_P values are from the cited literature and the X's from this work. The slopes of the curves (b) give an indication of the effective pressure P_t of the expanding gas.

are respectively 0.02 and 2×10^{-5} s. Applied to our present experiments, these items operate to establish the equilibrium $N_2O_4 \rightleftharpoons 2NO_2$ almost immediately after the sample enters the main nozzle part and to reestablish it in the nozzle capillary following the very small temperature drop the sample experiences on entering it. Upon emerging from the nozzle tip, the gas expands so rapidly that the number of molecular collisions are insufficient to alter the equilibrium appreciably before the gas reaches the scattering region. The composition of the system sampled in the scattering region is thus one that has been established by the "freezing" of the equilibrium at some point upstream.

These results are especially pleasing in the cases of conformational equilibria in which P_t plays no role, for they imply that T is well-known despite gas expansion. However, there are many reasons why the results might not all be applicable to other monomer−dimer equilibria. Most important is the question of whether the equilibrium in question becomes established in the nozzle being used. This means that with nozzles having short sample-residence time, like the one used in the present work, which is functionally typical of those used in other laboratories, only very fast equilibria are suitable subjects. If this criterion is met, our conclusion that the effective temperature of the system is almost certainly only a few degrees below that of the nozzle tip should apply. However, the effective pressure P_t is a more difficult matter because it depends on reaction in the capillary portion of the nozzle assembly, where the sample-residence time is very much shorter than in the main nozzle tube. If, for example, some reaction occurs in the capillary, the monomer−dimer ratio and P_t will change; but in the event of no reaction here, P_t will represent conditions in the main tube. In either event, P_t will have to be determined in each case by experiments similar to the ones at constant temperature that we have described for $NO_2-N_2O_4$.

Since conclusions about monomer−dimer equilibria studied by GED depend so strongly on nozzle geometry, one may inquire as to what options about the latter offer advantage. A simple alternative would be an oven−capillary assembly fitted with a needle valve in place of the nozzle tube−capillary assembly used for the present work. This device would be useful for substances that have a slow rate of approach to equilibrium: the sample could be held at a selected temperature for sufficient time to reach equilibrium before being released by the needle valve. A more elaborate version might consist of a double oven joined by a modest opening, each component of which could be heated independently. With the source, say solid, sample in the first compartment, adjustment of its temperature would allow control of P_t. The effective sample temperature T could be controlled by the heating of the second compartment, which could again be fitted with a needle valve. Finally, it should be noted that there could well be catalytic effects derived from the material from which the nozzles or ovens are fabricated. These effects will modify any of the above suggestions.

Acknowledgment. This work was supported by the National Science Foundation under Grants CHE95-25381 and GP-27763X. We would like to thank Professor Kolbjørn Hagen for his help with the experiments.

Supporting Information Available: Tables of scattered intensity data for each experiment and detailed data of experimental conditions (18 pages). See any current masthead page for ordering information.

References and Notes

(1) For the latest in the Oregon State series see: Kazerouni, M. R.; Hedberg, L.; Hedberg, K. *J. Am. Chem. Soc*. **1997**, *119*, 8324.

(2) Trongmo, O.; Shen, Q.; Hagen, K.; Seip, R. *J. Mol. Struct.* **1981**, *71*, 185.

(3) Gallaher, K. L.; Bauer, S. H. *J. Phys. Chem.* **1974**, *78*, 2380.

(4) Ryan, R. R.; Hedberg, K. *J. Chem. Phys.* **1969**, *50*, 4986.

(5) Shen, Q. Ph.D. Thesis, Oregon State University, 1974.

(6) (a) Hagen, K.; Hedberg, K. *J. Am. Chem. Soc.* **1973**, *95*, 1003. (b) Gundersen, G.; Hedberg, K. *J. Chem. Phys.* **1969,** *51*, 2500. (c) Hedberg, L. *Abstracts of Papers, Fifth Austin Symposium on Gas-Phase Molecular Structure;* Austin, TX, March 1974, p 37.

(7) Schäfer, L.; Yates, A. C.; Bonham, R. A. *J. Chem. Phys.* **1971**, *55*, 3055.

(8) Blank, J. S. Ph.D. Thesis, Oregon State University, 1964.

(9) McClelland, B. W.; Gundersen, G.; Hedberg, K. *J. Chem. Phys.* **1972**, *56*, 4541.

(10) Hedberg, K.; Iwasaki, M. *Acta Crystallogr*. **1964**, *17*, 529.

(11) Bird, G. R.; Baird, J. C.; Jache, A. W.; Hodgeson, J. A.; Curl, R. V.; Kunkle, A. C.; Bransford, J. W.; Rastrup-Andersen, J.; Rosenthal, J. *J. Chem. Phys.* **1964**, *40*, 3378.

(12) Giauque, W. F.; Kemp, J. D. *J. Chem. Phys.* **1938**, *6*, 40.

(13) Wourtzel, E. *Comptes Rendus* **1919**, *169*, 1397.

(14) Vosper, A. J. *J. Chem. Soc. (A)* **1970**, 625.

(15) Hisatsune, I. C. *J. Phys. Chem*. **1961**, *65*, 2249.

(16) A partial exception to this rule may exist in molecules with vibrational modes of very low frequency; these modes may relax somewhat more than others during the initial expansion of the sample as it leaves the nozzle capillary so that equipartition of the vibrational energy is upset.

(17) Yost, D. M.; Russel, H., Jr. *Systematic Inorganic Chemistry*; Prentice Hall: New York, 1944; Chapter 1.